Microrheological studies reveal semiflexible networks in gels of a ubiquitous cell wall polysaccharide

R. R. Vincent,[1,2] D. N. Pinder,[1] Y. Hemar,[1] and M. A. K. Williams[1,2,*]
[1]*Institute of Fundamental Sciences, Massey University, New Zealand*
[2]*MacDiarmid Institute for Nanotechnology and Advanced Materials, New Zealand*
(Received 28 March 2007; revised manuscript received 28 May 2007; published 11 September 2007)

Microrheological measurements have been carried out on ionotropic gels made from an important cell wall polysaccharide, using diffusing wave spectroscopy and multiple particle tracking. These gels were formed by the interaction of calcium ions with negatively charged groups on the polymer backbone, which is a copolymer of charged and uncharged sugars, galacturonic acid, and its methylesterified analog, respectively. The results suggest that semiflexible networks are formed in these systems, with a low frequency, frequency independent storage modulus ($G' > G''$), and a high frequency scaling of both G' and G'' with $\omega^{3/4}$. The differences observed between gels obtained using polysaccharide samples with different amounts and patterns of the charged ion-binding groups could comfortably be accommodated within this theoretical framework, assuming that the elementary semiflexible elements of the network are filaments consisting of two polymer chains bridged with calcium. In particular, a sample that was engineered to possess a blockwise intramolecular distribution of calcium chelating moieties clearly exhibited the high frequency scaling of both moduli with $\omega^{3/4}$ across some three orders of magnitude, and the concentration dependences of the elastic modulus, at both high and low frequency, were found to follow power laws with predicted exponents. Furthermore, quantitative agreement of the moduli with theory was found for realistic estimates of the molecular parameters, suggesting that the physics of semiflexible networks is not only exploited by protein components of the cytoskeleton but also by polysaccharides in plant cell walls.

DOI: 10.1103/PhysRevE.76.031909 PACS number(s): 87.16.Ka, 82.35.Pq, 83.80.Mc, 83.85.Ei

I. INTRODUCTION

It is well known that a plethora of biologically relevant soft materials exhibit heterogeneous hierarchical architectures that arise naturally from the propensity of constituent biopolymers to self-assemble and aggregate. These assembly processes can yield specific supramolecular structures, such as rods, helices, ribbons, and tubules, and in soft biomaterials of which they form a part it is predominantly the nature and interaction of these structural elements that mediate the storage and dissipation of mechanical energy. Thus, in order to understand the mechanical properties of this important class of soft materials it must be appreciated that, in contrast to classical rubberlike networks of flexible chains connected by pointlike crosslinks, many biopolymer systems are assembled from semiflexible filaments that can have a persistence length in excess of the distance between entanglements [1,2]. This means, among other things, that the mechanical response of such systems may include a significant elastic contribution from bending modes and that networks easily strain harden, a fact that presumably played no small part in the success of such evolved strategies in biomaterials.

Throughout the last decade, bolstered by progress in the development of microrheological techniques [3–12], a series of seminal works on *F*-actin, an important filament-forming protein of the cytoskeleton, have been carried out [13–29]. Indeed, *F*-actin has been the exemplary system studied by physicists working on network theories of semiflexible polymers and excellent progress in both experimental and theoretical aspects have been made using this system.

More recently, strain hardening has been demonstrated to be a common feature of many biopolymeric systems, originating from the semiflexible nature of network strands [30], and an extensive set of rheological data for the biopolymer gelatin has been interpreted within the same framework, in which renatured stiff triple helices form the elementary network elements [31]. While strain hardening has been reported experimentally in a number of polysaccharide gels [32], there has been no published interpretation of this behavior and further, to our knowledge, there has been no convincing demonstration that the same underlying physics demonstrated to play such an important role in proteinaceous systems may also govern the behavior of soft polysaccharide based materials.

In this work the mechanical properties of ionotropic gels of the polysaccharide pectin are studied. Pectin is found in the cell walls of all land plants and although this is a complex biological matrix in which hemicelluloses, pectins, cellulose, proteins, and lignin all play a role in determining structure and properties, it is known that the pectin component has considerable mechanical utility within the cell wall, in which the binding of calcium plays a significant role [33,34]. Pectin is extracted commercially from lemon peel and apple pomace and consists mainly of 1,4 linked α-*D*-galacturonate residues (typically ~90%). This dominant part of the pectin, referred to as homogalacturonan, is a linear and relatively stiff anionic polymer [35], and is responsible for the manifest ion binding. However, the sugar residue also naturally occurs in an uncharged, calcium-impotent, methylesterified form, as shown in Fig. 1(a). Pectins are usually characterized by this degree of methylesteri-

*m. williams@massey.ac.nz

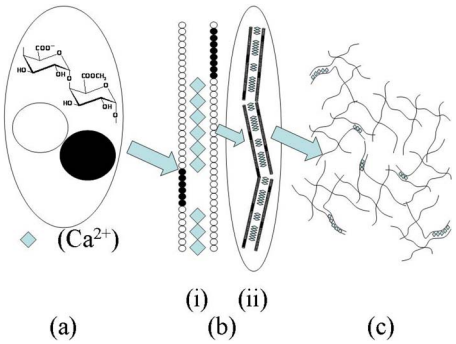

FIG. 1. (Color online) A schematic diagram of the proposed assembly process in ionotropic pectin gels. (a) Charged galacturonic acid residues and uncharged methylesterified analogs are represented by open and filled circles, respectively. (b) (i) Galacturonic acid residues on neighboring chains zip-up with calcium ions, represented by diamonds, and (ii) forming stiff fibrils. (c) Interfibrillar crosslinks may also be formed with calcium depending on the amount of calcium available.

fication (DM) and their network formation capabilities are clearly related to this value, with DM $<50\%$ pectins forming ion-induced networks *in vitro*. Interestingly, this structural feature is known to be modified *in vivo* as the plant engineers its constituent polymers, eliciting desired mechanical changes in order to facilitate varied physiological processes.

Broadly, calcium-induced pectin networks are formed according to a so-called egg box model [36] in which gelation proceeds in two steps. The first step is a rapid formation of dimeric junction zones where calcium is chelated between the negatively charged carboxyl groups of two pectin chains, as shown schematically in Fig. 1(b). Subsequent dimer-dimer aggregation, as depicted in Fig. 1(c) may also occur when there is sufficient calcium present. It is believed that the formation of a stable junction zone requires a block of approximately 12–16 consecutive free galacturonic acid (GalA) units along the polymer backbone [36,37]. Hence, the *in vitro* and *in vivo* interaction with calcium ions, and the properties of the gels thereby formed, are expected to depend not only on the amount of ion-binding groups possessed by the polymer, but also on the distribution of such groups along the backbone.

Although pectin gels are not traditionally considered to be particularly filamentous in character the individual polymers are themselves semiflexible, with persistence lengths of around 15 sugar residues compared with a contour length of some 200–500 [38]. Furthermore, their polyelectrolytic nature and the postulated increased stiffness of calcium-crosslinked dimers makes them interesting model systems. In addition, by modifying the concentration and fine structure of the polymer, changes to the phase volume, and entanglement and persistence lengths of constituent dimers can be made, and the consequences examined.

II. EXPERIMENTAL DETAILS

Materials

Pectins ($M_w \sim 150$ kDa), extracted from citrus peel with galacturonic contents of $\sim 90\%$, and sample average degrees of methylesterification of 35% and 86% were kindly supplied by CP Kelco ApS, DK 4623 Lille Skensved, Denmark. The first sample was produced in-house by deesterification of a highly methylesterified pectin with a fungal enzyme, which, owing to its mode of action, produces a random arrangement of calcium binding groups along the polymer backbone. The second, highly esterified sample, was used to prepare (i) a 48% DM sample, made using a base saponification in order to produce a random distribution of charged residues, and (ii) a 50% DM sample, produced using a processive commercial pectin methyl esterase (PME) [EC 3.1.1.11] purchased from Sigma Aldrich (P5400) to remove the methylester groups and hence generate a highly blockwise charge distribution [39].

The sample average DMs of all the samples were determined using capillary zone electrophoresis (CE) as previously described [39–41]. In order to verify the differences in the intramolecular distribution of the calcium binding groups the polymers were incubated with a polygalacturonase [EC 3.2.1.15] that was kindly provided by Jacques Benen from the University of Wageningen. This is a pure endo-PG II isoform from *Aspergillus Niger* [42] and has an absolute requirement for the sugar residues in the active site to be unesterified in order for the chain to be severed, which yields the degradation pattern methylester-sequence dependent. Digest fragments were monitored using CE [43–45]. Large amounts of mono-, di-, and tri-galacturonic acid were liberated by the endo-PG II digest of the PME generated sample and in concert with the lack of detectable partially methylesterified low degree of polymerization fragments, these observations confirm its blockwise nature.

For microrheology experiments stock pectin solutions of 1–3% w/w were prepared by dissolving the pectin powder in water (minimum resistance 18.2 MΩ) and stirring overnight. The pH was adjusted to 5.6 with a solution of 0.1 M NaOH, in order to ensure that the unmethylated galacturonic residues were fully charged ($pK_a \sim 3.5$).

$CaCO_3$ powder with a mean particle diameter of 1 μm was kindly provided by Provencale s.a., Avenue Frédéric Mistral, 83172 Brignoles Cedex, France. Glucono-δ-lactone (GDL) was purchased from Fisher Scientific, Bishop Meadow Rd., Loughbourough, LE11 5RG, UK. Latex particles of diameter 465 nm (2.62% w/v stock solutions) and fluorescent particles of diameter 541 nm (Fluoresbrite plain YG, 2.64% w/v stock solution) were purchased from Polyscience Inc. (Warrington, PA).

Sample preparation

Pectin gels. Ionotropic pectin gels were obtained by slowly releasing calcium ions into pectin solutions [46] containing 1% w/v of latex beads (DWS) or 0.03% w/v of fluorescent beads (MPT). The appropriate amounts of pectin and bead stock solutions were mixed and stirred, and immediately prior to loading into appropriate test cells a salt solution was added, the final mixing of which achieves the final desired concentration of all components of the system.

This aqueous salt solution was composed of $CaCO_3$ and GDL. The GDL hydrolyzes with time, releasing protons that solubilize calcium ions from the $CaCO_3$. These components were introduced as powders into water, quickly mixed, and added to the pectin-bead solution as quickly as possible, in order to avoid significant calcium release before mixing with pectin. The quantity of $CaCO_3$ added determines the R value, $R=2^*[Ca^{2+}]/[COO^-]$ which can, by controlling the amount and extent of interchain association, be varied to tune the elasticity of the material. A stoichiometric ratio of GDL $[GDL]=2^*[Ca^{2+}]$ is used in order to maintain the pH of the solution [46]. After the addition of the salts the final prepared solution was stirred for a few minutes, and the samples were loaded on the appropriate test cell and left overnight.

Microrheology

The aim of microrheology is to extract the rheological properties of soft materials from the motion of probe particles immersed in the material [47]. Passive microrheology, contrary to active microrheology, is the simple study of the particle's thermal motion. It is a nondestructive technique and recovers the linear response of the material, in contrast to active microrheology. For a viscoelastic fluid, the mean square displacement (MSD) of a probe particle will vary as a local power law $\langle \Delta r^2(\tau)\rangle \sim \tau^\alpha$ with $0 \leq \alpha \leq 1$ depending on the nature of the medium, and τ is the observation time. In order to link the measured MSD to the viscoelastic properties, a generalized Stokes-Einstein relation (GSER) [10] can be used with the caveats that the fluid is incompressible and the boundary nonslip.

$$\hat{G}(s) = \frac{k_B T}{\pi a s \langle \hat{\Delta} r^2(s)\rangle}, \tag{1}$$

with $\hat{G}(s)$ the shear modulus in the Laplace space, s the Laplace frequency, and $\langle \hat{\Delta} r^2(s)\rangle$ the Laplace transform of the MSD. The complex shear modulus $G^*(\omega)$ is the Fourier transform of $G(t)$, with ω the Fourier frequency. A numerical method for determining the elastic (G') and viscous (G'') shear moduli from the MSD has been detailed by Mason [10]. The storage and loss moduli are given as a function of the frequency ω by:

$$G(\omega) = \frac{k_B T}{\pi a \langle \Delta r^2(1/\omega)\rangle \Gamma[1+\alpha(\omega)]}, \tag{2}$$

$$G'(\omega) = G(\omega)\cos[\pi a(\omega)/2], \tag{3}$$

$$G''(\omega) = G(\omega)\sin[\pi a(\omega)/2]. \tag{4}$$

$\langle \Delta r^2(1/\omega)\rangle$ is the MSD at time $\tau = 1/\omega$, $\alpha(\omega) = |\partial \ln\langle \Delta r^2(\tau)\rangle / \partial \ln \tau|_{\tau=1/\omega}$, and Γ is the gamma function. We used this method and an extension in which second order derivatives are also taken in order to better characterize the local power laws [10,48].

DWS experimental arrangement

The DWS apparatus used in this study has been fully described previously [49]. The samples were contained in glass cells of width 10 mm, height 50 mm, and path length L of 4 mm, and were illuminated with a 35 mW HeNe Melles-Griot laser operating at wavelength $\lambda = 633$ nm. The laser beam was expanded to approximately 8 mm on the surface of the cell. The transmitted scattered light was detected using a single-mode optical fiber (P1-3224-PC-5, Thorlabs Inc., Germany). The optical fiber was connected to a Hamamatsu HC120-08 PMT photomultiplier tube module, and the intensity autocorrelation functions of the scattered light were obtained using a Malvern 7132 correlator. Tests were run for 20 min to ensure low noise intensity autocorrelation functions.

For an expanded beam mode, the field autocorrelation function $g_1(t)$ is obtained from the measured intensity autocorrelation function $g_2(t)$ using the Siegert equation $g_2(t) = 1 + \beta g_1^2(t)$, where β is a constant depending on the instrument. In the transmission geometry, the field autocorrelation function is given by [50]

$$g_1(t) = \frac{\frac{L/l^* + 4/3}{z_0/l^* + 2/3}\left\{\sinh\left[\frac{z_0}{l^*}\sqrt{k_0^2\langle \Delta r^2(\tau)\rangle}\right] + \frac{2}{3}\sqrt{k_0^2\langle \Delta r^2(\tau)\rangle}\cosh\left[\frac{z_0}{l^*}\sqrt{k_0^2\langle \Delta r^2(\tau)\rangle}\right]\right\}}{\left(1+\frac{8t}{3\tau}\right)\sinh\left[\frac{L}{l^*}\sqrt{k_0^2\langle \Delta r^2(\tau)\rangle}\right] + \frac{4}{3}\sqrt{k_0^2\langle \Delta r^2(\tau)\rangle}\cosh\left[\frac{L}{l^*}\sqrt{k_0^2\langle \Delta r^2(\tau)\rangle}\right]}, \tag{5}$$

where l^* is the scattering mean free path, z_0 is the penetration depth (assumed here to equal l^*), $k_0 = 2\pi/\lambda$, and L is the sample thickness (4 mm here). l^* is obtained by performing an experiment on a water sample using 1% of latex beads, and fitting l^* using the accepted viscosity. Subsequently, l^* for future samples is obtained by scaling the value obtained for water, based on the change in transmitted intensity when the sample is introduced, compared to the water experiment. It is known that for nonabsorbing slabs of thickness L, the transmitted intensity is directly proportional to $(l^*/L)(1+4l^*/3L)$, so that by measuring the change in transmittance, the change in l^* can be calculated [50]. Once l^* is

determined, the MSD can be obtained from the experimental correlation functions by inverting Eq. (5) with a zero-crossing routine.

MPT experimental setup

The Brownian motion of fluorescent polystyrene beads was monitored with an Olympus OH2 microscope, and using a 100× oil immersion lens. 45 frames s^{-1} were recorded with a UP800 CCD camera (UNIQVISION, USA), typically for 20 s, and digitalized with a PCDIG L frame grabber (Dalsa Coreco, CA). The motions of approximately 40 particles were determined using the tracking software in Image-Pro Plus (Media-Cybernetics, USA), in order to obtain the MSD as a function of observation time. The one-point MSD was obtained by averaging over all the particles and all the initial times as follows:

$$\langle \Delta r^2(\tau) \rangle_{OPMR} = \langle [r_\alpha(t+\tau) - r_\alpha(t)]^2 \rangle_{t,\alpha}, \quad (6)$$

where $r_\alpha(t)$ is the position of the particle α at time t, and τ, the lag time.

Our microrheological setups were thoroughly tested using glycerol-water mixtures of known viscosities and an archetypal flexible polymer, polyethylene oxide (PEO), and were shown to perform well in both cases [51].

III. RESULTS AND DISCUSSION

Figure 2(a) shows the mean square displacement of tracer particles as a function of time, as measured by DWS and MPT, when embedded in a calcium-induced gel made with a commercially available pectin sample. These initial experiments were carried out at a polymer concentration of 1% w/w using a sample with some 65% of the sugar residues charged and randomly distributed along the backbone, the gel being formed as described in the experimental section. The agreement between the techniques is good. In addition to supporting the DWS data, the MPT measurements also allow the spatial heterogeneity of the mechanical properties [11,20,52–54] to be assessed and it should be noted that Van Hove correlation functions for this system, and indeed all those described herein, were Gaussian and indicated that there was no significant difference in the local rheological properties experienced by the individual tracer particles, so that quantitative microrheology could safely be performed. Further work on this aspect of the gels in different concentration regimes will be reported elsewhere.

There is a striking resemblance between these one-point microrheological results and work reported on actin solutions [7,17,18,29]. Motivated by this obvious similarity we endeavored to fit our one-point MSD to the theoretical expression used in the actin work [29]. The theoretical MSD for a small bead that couples to single filament eigenmodes that are themselves coupled to collective modes of an overdamped elastic background is predicted to have the form

$$\Delta x^2(t) = A\{1 - (\pi/t)^a \, \mathrm{erf}(t^a)/2\} + B\{1 - bt^b \Gamma[-b,t]\}, \quad (7)$$

where $a=1/2$, $b=3/4$, t is in units of τ_c, erf is the error function, and Γ is the incomplete gamma function. The fit of

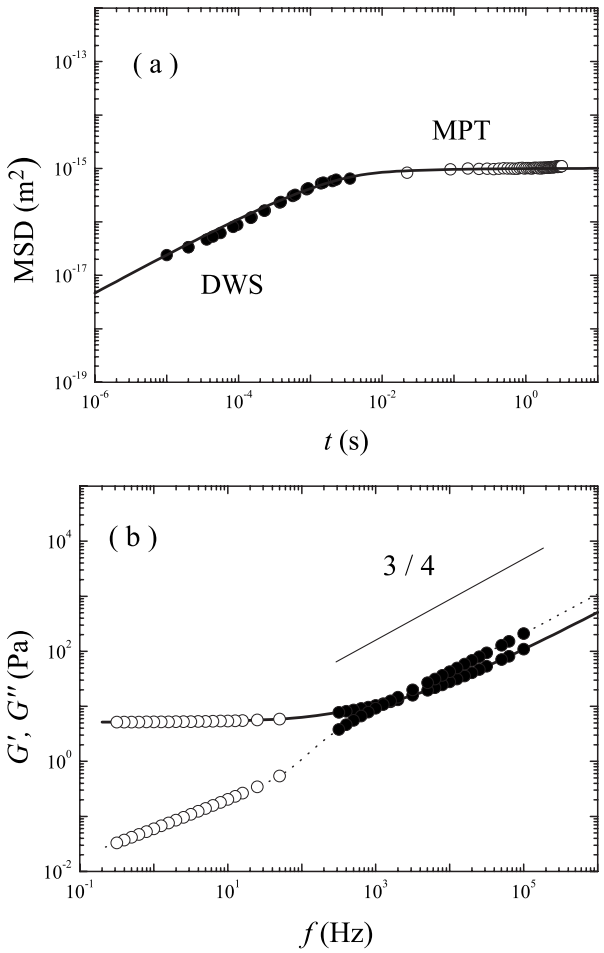

FIG. 2. (a) The MSDs obtained from experiments using DWS (filled circles), and multiple particle tracking (open circles), on an ionotropic gel of the polysaccharide pectin formed as described in the Experimental section. The solid line is a fit to a theoretical model, described in the text. (b) The viscoelastic properties obtained from the transformation of this data. The solid and dotted guidelines show G' and G'', respectively, both scaling with $\omega^{3/4}$ at high frequencies.

the one-point DWS and MPT data, to this functional form is shown in the figure. Given the good agreement in the time domain it is unsurprising to find that the viscoelastic properties we obtain from the transformation of this data, also closely resemble that previously reported, in particular, giving both elastic and viscous moduli (G' and G'') scaling with $\omega^{3/4}$ at high frequencies [Fig. 2(b)]. Although the adherence to the 3/4 scaling within the data range of these preliminary experiments is clearer for G'' than G', the power law dependence of the elastic modulus is clearly revealed in the frequency response obtained by transforming the extrapolated time domain fitting function. Furthermore, the switch to a frequency independent elastic modulus at low frequencies also looks extremely similar to recent data obtained on lightly crosslinked actin filaments [28]. It is worth clarifying that experiments carried out on pectin solutions in the absence of calcium show that there is no tendency for the MSDs to exhibit a high frequency 3/4 scaling of the moduli; crosslinks are not introduced between preexisting filaments

as in the actin study [28] but rather we will argue that semiflexible filaments are generated by the addition of calcium [shown schematically in Fig. 1(b)], which can also lightly crosslink some filaments [Fig. 1(c)]. To summarize, initial experiments carried out using a commercially available pectin sample with 65% of the backbone sugar residues charged and randomly distributed along the backbone, were suggestive that the calcium-induced gels formed from such systems were lightly crosslinked entangled semiflexible networks, with a low frequency, frequency independent elastic modulus ($G' > G''$) and a high frequency scaling of both G' and G'' with $\omega^{3/4}$.

In order to investigate this behavior further, and, in particular, to gather additional evidence that the scaling power of 3/4 arises from the redistribution of bending modes of individual filaments induced on compression or stretching, we examined systems in which existing molecular engineering skills were exploited in order to generate systems in a similar regime but where the persistence length of constituent fibrils was varied. Unlike actin systems where the relationships between the polymer concentration and filament density, and filament length and persistence length are reasonably straightforward, owing to the fact that all the polymer is incorporated into the semiflexible filaments, in pectin systems the situation is not so clear cut. In these copolymeric systems only the charged (unmethylesterified) groups have the potential to bind the calcium into junction zones, postulated to be the semiflexible filaments of the network, as shown in Fig. 1(c). Furthermore, it has been proposed that a minimum length of sequential ion-binding groups is required to form stable calcium mediated bridges, which renders the pattern of methylesterification crucial to the ability of a particular region of the polysaccharide backbone to participate in a calcium chelation zone or filament motif. Further still, the consequences of interspersing different lengths of "mismatched regions" containing methylesterified groups into otherwise calcium binding runs of charged sugars are not clear. While the bending modulus of the filament is likely to vary spatially along the chain if multiple lengths of calcium bound stiff dimeric regions are interrupted by methylester groups, defining whether or not such regions are "part of a filament" is not trivial. In addition, chain to chain variation in the degree of methylesterification also exists, and although measurements of this can be made [39,40], it further complicates the matter in hand.

Despite the complexities of the exact relationship between filament properties and polymeric fine structure it is clear nevertheless that the amount and pattern of ion-binding groups on the backbone are likely to give rise to changes in both the filament density and average persistence length. Hypothesizing that polymer dimers cross-linked with calcium do essentially form the fundamental filamentary elements of the network, experiments were subsequently carried out using polymer architectures that were engineered to possess (1) less calcium binding groups and (2) a more blockwise intramolecular distribution of ion-binding groups, when compared to the pectin used in the preliminary studies. While the former would be expected to possess smaller average persistence lengths of filaments, the latter would be expected to form longer, stiffer dimers. Furthermore, having the ion-binding groups arranged blockwise ameliorates some of the difficulties described above thereby simplifying the estimation of the filament density. Such blockwise fine structures are also considerably closer to native structures found in plant cell walls.

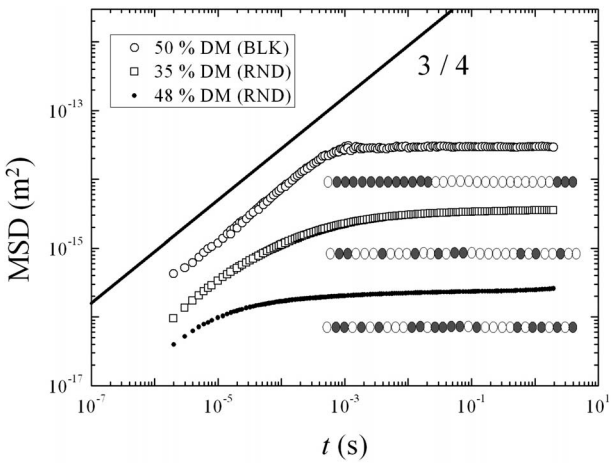

FIG. 3. The MSDs obtained from experiments using DWS on ionotropic gels of pectin samples with different backbone architectures. Samples of 35 and 48% DM having randomly distributed ion-binding groups (open circles in the schematic polymer structures inset), and a 50% DM sample possessing a blockwise distribution of charged groups are shown. These were formed as described in the experimental section (●) 1.5% w/w polymer, $R=0.4$; (□) 1% w/w polymer, $R=0.3$; (○) 0.2% polymer, $R=0.4$).

Figure 3 shows the mean square displacement of the thermally activated movement of tracer particles, measured by DWS, in pectin gels made from polysaccharides engineered to have different amounts and patterns of ion-binding groups as described in the experimental section. While the polymer and calcium concentrations have also been controlled in order to satisfy a number of practical considerations regarding the gel formation, the significance of which will be addressed in due course, a number of points are nevertheless clear. For a random distribution of ion-binding groups the 3/4 power law behavior moves to higher frequencies as the number of ion-binding groups is reduced, while for a blockwise distribution where all the calcium chelating groups are able to participate in junction zone formation the semiflexible network signature is clearly observable over nearly 3 orders of magnitude in time (from $\sim 10^{-6}$ to $\sim 10^{-3}$ s). This strongly suggests that indeed the elastic and viscous moduli (G' and G'') scaling with $\omega^{3/4}$ at high frequencies observed in pectinacious systems reflects the semiflexible nature of network filaments that consist of calcium crosslinked polymer chains.

Not only does the sample possessing the blockwise charge distribution exhibit the clearest signatures of semiflexible behavior but, as described above, it is the easiest sample to model, where the assumption that all ion-binding groups have the potential to be part of a filament is likely to be a reasonable approximation. Bearing this in mind, as well as the intrinsic interest in its biomimetic connection, we carried out further studies on this sample. Figure 4 shows the measured MSDs of the tracer particles in calcium mediated gels

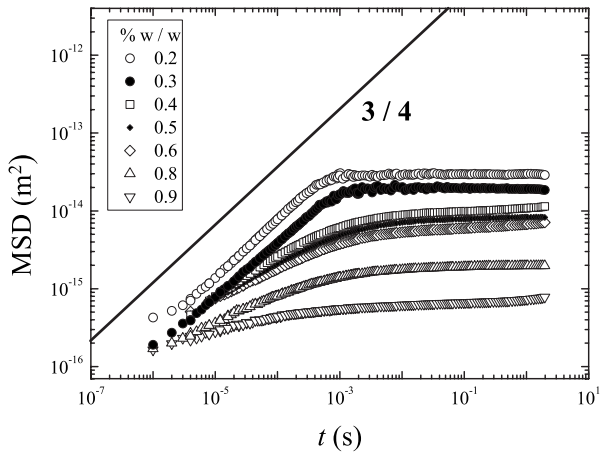

FIG. 4. The MSDs obtained from experiments using DWS on ionotropic gels of pectin samples with 50% ion-binding groups arranged in a blockwise distribution, formed as described in the Experimental section, as a function of concentration.

of this blockwise sample at various polymer concentrations. The theoretical framework of the semiflexible network model also provides predictions for the scaling exponent of the elastic moduli (or equivalently the MSD) with concentration at both high and low frequencies [2] and the data obtained in our experiments at 10^{-4} and 10^{-1} Hz are shown in Figs. 5(a) and 5(b), where it can be seen that for concentrations below 0.8% w/w the agreement is good (1.03±0.05 cf. 1 and 1.5±0.1 cf. 1.4, respectively). This provides further evidence of the governing semiflexible network physics in this regime. Above this concentration agreement with the concentration dependence predicted by this model is lost. It can be noted that concurrently it is at these concentrations in Fig. 4 that the measured data no longer show a clear asymptotic trend towards a scaling of 3/4 at high frequency, in good agreement that at these concentrations we are entering a regime in which the network behavior is dominated by another factor that we suggest to be the bundling of dimeric filaments. It is also worth noting that the comparison of these results reported in Fig. 4 with those obtained using different polymeric fine structures (Fig. 3) confirms the hypothesis that differences in the latter cannot be explained solely by the differences in concentration of the samples that were necessitated by practical issues regarding the kinetics of gel formation, and reflect a significant contribution from variations in filament length.

Finally, still further evidence is presented in the form of a calculation of the moduli at high frequency based on the estimation of molecular parameters in the regime where we are claiming semiflexible network physics is governing the mechanical properties. In order to compare the calculation of mechanical properties with the experimental data, the measured MSD for the 0.2% w/w blockwise sample was transformed to the frequency domain as described in the Experimental Details. It should be noted that in order to perform the numerical derivatives the time domain data is routinely fitted to a smooth functional form, such as double or reciprocal power laws [52,55]. While the results shown in Fig. 2 suggest a fit to Eq. (7) would be useful in this regard we

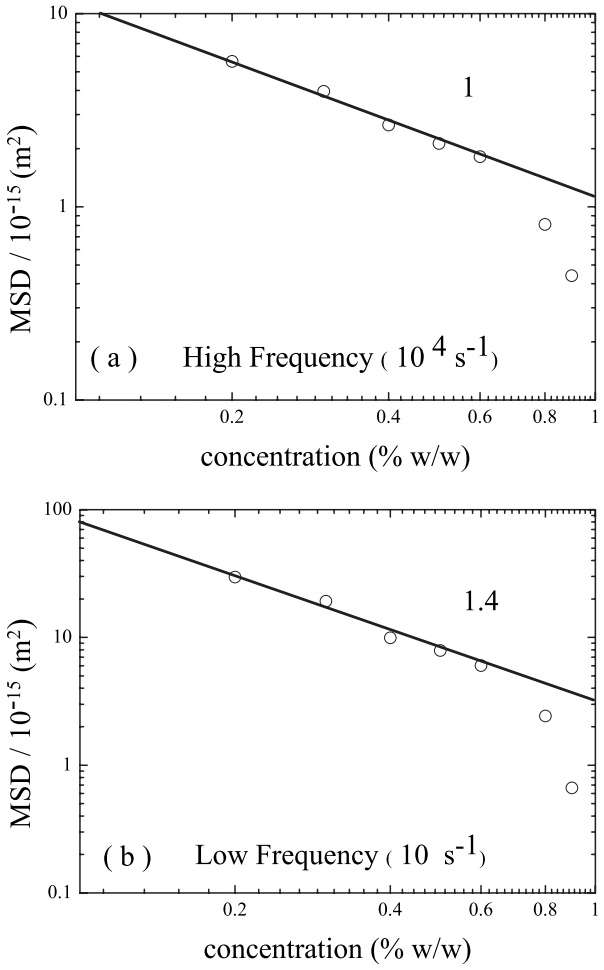

FIG. 5. The concentration dependence of the mean square displacements of tracer particles in a 0.2% w/w gel of the 50% DM, PME generated, pectin. (a) At high frequency and (b) at low frequency.

found that while the proposed form certainly captures the main features of the 0.2% data it struggled to reproduce the transition region in detail. The experimental points fell below the prediction at long times, as found previously in actin studies [29], but also were significantly above the theory in the transition region (not shown). The results of an MPT experiment were consistent with the measured long time displacement, and taken with the good agreement of this data with the concentration dependence of the MSDs shown in Fig. 5, there is reasonable experimental evidence supporting the sharpness of the measured low frequency cutoff. Therefore, in lieu of a physically significant functional form that captures the detail of the measured MSD across the whole measured time domain, a transform was carried out simply in the asymptotic regions. Figure 6 shows the experimental data transformed as described and the results of a theoretical calculation performed using [2]

$$G(\omega) = \frac{1}{15}\rho\kappa l_p(-2i\varsigma/\kappa)^{3/4}\omega^{3/4} - i\omega\eta, \tag{8}$$

where ρ is the polymer concentration in length per unit volume, κ is the bending modulus, l_p is the persistence length,

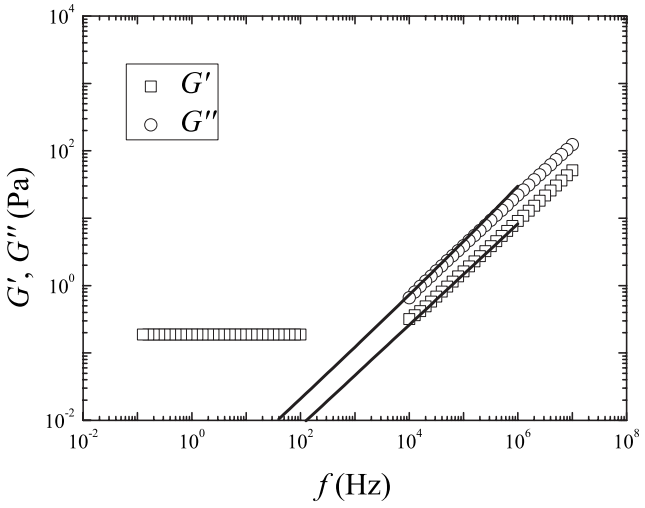

FIG. 6. The frequency dependence of G' and G'' measured on a 0.2% w/w gel of the 50% DM, PME generated, pectin. The solid line is a theoretical calculation performed as described in the text.

and ζ is the lateral drag coefficient per unit length, which we have approximated by $4\pi\eta/\ln(\varepsilon/a)$, where η is the viscosity, ε is the mesh size, and a is the radius of the filament.

By assuming the filament radius is of the order of 1 nm (which seems reasonable for a dimeric polysaccharide), and that the filament density can be calculated from the actual polymer concentration multiplied by the fraction of sugars that are charged (0.5) and by the fraction of those that have available calcium (0.4) then at 293 K and at a polymer concentration of 0.2% w/w the quantitative prediction is shown in Fig. 6, assuming a filament persistence length of some 300 nm [2,28]. This filament persistence length is not unreasonable based on available microscopy of similar pectin systems [56], although it is the order of the chain contour length and is only a factor of 3 larger than the predicted mesh size. While this set of molecular parameters seem at least reasonable for an order of magnitude calculation, the lateral drag coefficient required in order to then produce the shown prediction is some two orders of magnitude less than that found for *F*-actin [28]. This in itself it perhaps not surprising, although calculating this value from the approximation given above seems to require a physically unrealistic viscosity of the medium exerting drag on the filaments of 0.01 mPas. On the whole, considering the approximations made for this highly complex system, the calculation serves to show that it is not unreasonable that indeed these gels of structural anionic polysaccharides exhibit a regime in which their mechanical response is governed by the physics of semiflexible networks. Although the plant cell wall is an extremely complex biopolymer matrix, as discussed, the positioning of this regime in terms of polymer and calcium concentration suggest that this may be operative *in vivo* [33,57].

IV. CONCLUSION

The anionic polysaccharide pectin is a crucial structural component in the cell walls of all land plants where it is, amongst other things, crosslinked with calcium ions. *In vitro* microrheological characterization of calcium-induced pectin gels revealed a regime that exhibits the signatures of lightly crosslinked, entangled semiflexible networks, with a low frequency, frequency independent elastic modulus ($G' > G''$) and a high frequency scaling of both G' and G'' with $\omega^{3/4}$. Experiments subsequently carried out using polymer architectures in which the degree of calcium mediated association could be altered suggest that pectin chains crosslinked with calcium form the fundamental filamentary elements of the network. In particular, a pectin sample was modified by a plant enzyme in order to produce a more blockwise intramolecular distribution of ion-binding groups and when ionotropic gels were made using this polymer the predicted semiflexible scaling regime was clearly observed over almost three orders of magnitude. Furthermore, the concentration dependence of the MSDs obtained from this sample, at both high and low frequency, followed power laws with exponents predicted within the theoretical framework of semiflexible networks; and quantitative agreement of the moduli with theory was found for realistic estimates of the molecular parameters.

While such a regime has been extensively investigated for other semiflexible biopolymers, in particular, *F*-actin and other intermediate filaments of the cytoskeleton, this is the first time that experimental evidence has been reported suggesting that the same underlying physics may be applicable to a polysaccharide system. This work therefore suggests that the semiflexible network model may have utility beyond protein filament gels, in the study of polysaccharide-based soft materials with much smaller mesh sizes and persistence lengths. Furthermore, these findings suggest that it is possible that the same semiflexible network physics that provides the mechanical framework of the cytoplasm, may also have a role to play in understanding the cell wall. Interestingly, the polymer and calcium concentrations spanning this regime could well be representative of certain cell wall types under physiologically relevant conditions. Future work will include the investigation of the transition to bundling at higher concentrations, strain hardening phenomena, and the effects of the presence of other components such as cellulose microfibrils, in an attempt to move towards a mechanical understanding of more realistic cell wall mimics.

ACKNOWLEDGMENTS

The authors gratefully acknowledge the MacDiarmid Institute for Advanced Materials and Nanotechnology for the funding of a Ph.D. studentship (R.R.V.). The CCD camera used in this work was purchased with assistance from the Institute of Fundamental Science Graduate Research Fund (IFSGRF). We would like to thank Anna Ström and Aurélie Cucheval for assistance in manipulation of the polymeric architectures and Professor F. MacKintosh for encouragement and helpful comments.

[1] K. Kroy, Curr. Opin. Colloid Interface Sci. **11**, 56 (2006).
[2] F. C. MacKintosh, in *Soft Condensed Matter Physics in Molecular and Cell Biology*, edited by W. C. K. Poon and D. Andelman (Taylor & Francis, London, 2006).
[3] D. J. Pine, D. A. Weitz, P. M. Chaikin, and E. Herbolzheimer, Phys. Rev. Lett. **60**, 1134 (1988).
[4] T. G. Mason and D. A. Weitz, Phys. Rev. Lett. **74**, 1250 (1995).
[5] J. C. Crocker and D. G. Grier, J. Colloid Interface Sci. **179**, 298 (1996).
[6] T. G. Mason, K. Ganesan, J. H. van Zanten, D. Wirtz, and S. C. Kuo, Phys. Rev. Lett. **79**, 3282 (1997).
[7] F. Gittes, B. Schnurr, P. D. Olmsted, F. C. MacKintosh, and C. F. Schmidt, Phys. Rev. Lett. **79**, 3286 (1997).
[8] T. G. Mason, A. Dhople, and D. Wirtz, *MRS Proceedings on Statistical Mechanics in Physics and Biology*, Vol. 463, p. 153 (1997).
[9] T. G. Mason, H. Gang, and D. A. Weitz, J. Opt. Soc. Am. A **14**, 139 (1997).
[10] T. G. Mason, Rheol. Acta **39**, 371 (2000).
[11] M. T. Valentine, P. D. Kaplan, D. Thota, J. C. Crocker, T. Gisler, R. K. Prud'homme, M. Beck, and D. A. Weitz, Phys. Rev. E **64**, 061506 (2001).
[12] D. T. Chen, E. R. Weeks, J. C. Crocker, M. F. Islam, R. Verma, J. Gruber, A. J. Levine, T. C. Lubensky, and A. G. Yodh, Phys. Rev. Lett. **90**, 108301 (2003).
[13] F. C. MacKintosh, J. Käs, and P. A. Janmey, Phys. Rev. Lett. **75**, 4425 (1995).
[14] D. C. Morse, Phys. Rev. E **58**, R1237 (1997).
[15] B. Schnurr, F. Gittes, F. C. MacKintosh, and C. F. Schmidt, Macromolecules **30**, 7781 (1997).
[16] F. Gittes and F. C. MacKintosh, Phys. Rev. E **58**, R1241 (1998).
[17] J. Xu, V. Viasnoff, and D. Wirtz, Rheol. Acta **37**, 387 (1998).
[18] J. Xu, A. Palmer, and D. Wirtz, Macromolecules **31**, 6486 (1998).
[19] A. Palmer, J. Y. Xu, and D. Wirtz, Rheol. Acta **37**, 97 (1998).
[20] J. Apgar, Y. Tseng, E. Fedorov, M. B. Herwig, S. C. Almo, and D. Wirtz, Biophys. J. **79**, 1095 (2000).
[21] T. G. Mason, T. Gisler, K. Kroy, E. Frey, and D. A. Weitz, J. Rheol. **44**, 917 (2000).
[22] P. Dimitrakopoulos, J. F. Brady, and Z. G. Wang, Phys. Rev. E **64**, 050803(R) (2001).
[23] L. LeGoff, O. Hallatschek, E. Frey, and F. Amblard, Phys. Rev. Lett. **89**, 258101 (2002).
[24] M. L. Gardel, M. T. Valentine, J. C. Crocker, A. R. Bausch, and D. A. Weitz, Phys. Rev. Lett. **91**, 158302 (2003).
[25] M. L. Gardel, J. H. Shin, F. C. MacKintosh, L. Mahadevan, P. A. Matsudaira, and D. A. Weitz, Phys. Rev. Lett. **93**, 188102 (2004).
[26] I. Y. Wong, M. L. Gardel, D. R. Reichman, E. R. Weeks, M. T. Valentine, A. R. Bausch, and D. A. Weitz, Phys. Rev. Lett. **92**, 178101 (2004).
[27] M. L. Gardel, J. H. Shin, F. C. MacKintosh, L. Mahadevan, P. A. Matsudaira, and D. A. Weitz, Science **304**, 1301 (2004).
[28] G. H. Koenderink, M. Atakhorrami, F. C. MacKintosh, and C. F. Schmidt, Phys. Rev. Lett. **96**, 138307 (2006).
[29] J. Liu, M. L. Gardel, K. Kroy, E. Frey, B. D. Hoffman, J. C. Crocker, A. R. Bausch, and D. A. Weitz, Phys. Rev. Lett. **96**, 118104 (2006).
[30] C. Storm, J. J. Pastore, F. C. MacKintosh, T. C. Lubensky, and P. A. Janmey, Nature (London) **435**, 191 (2005).
[31] E. van der Linden and A. Parker, Langmuir **21**, 9792 (2005).
[32] C. Michon, C. Chapuis, V. Langendorff, P. Boulenguer, and G. Cuvelier, Food Hydrocolloids **18**, 999 (2004).
[33] S. C. Fry, *The Growing Plant Cell Wall: Chemical and Metabolic Analysis* (The Blackburn, Caldwell, 2000).
[34] W. G. T. Willats, P. Knox, and J. D. Mikkelson, Trends Food Sci. Technol. **17**, 97 (2006).
[35] E. R. Morris, D. A. Powell, M. J. Gidley, and D. A. Rees, J. Mol. Biol. **155**, 507 (1982).
[36] D. A. Powell, E. R. Morris, M. J. Gidley, and D. A Rees, J. Mol. Biol. **155**, 517 (1982).
[37] R. Kohn and O. Luknar, Collect. Czech. Chem. Commun. **40**, 959 (1975).
[38] S. Cros, C. Garnier, M. A. V. Axelos, A. Imberty, and S. Pérez, Biopolymers **39**, 339 (1996).
[39] M. A. K. Williams, T. J. Foster, and H. A. Schols, J. Agric. Food Chem. **51**, 1777 (2003).
[40] H. J. Zhong, M. A. K. Williams, D. M. Goodall, and M. Hanson, Carbohydr. Res. **308**, 1 (1998).
[41] H. J. Zhong, M. A. K. Williams, R. D. Keenan, and D. M. Goodall, Carbohydr. Polym. **32**, 27 (1997).
[42] H. C. M. Kester and J. Visser, Eur. J. Biochem. **259**, 577 (1996).
[43] M. A. K. Williams, G. M. C. Buffet, and T. J. Foster, Anal. Biochem. **301**, 117 (2002).
[44] A. Ström and M. A. K. Williams, Carbohydr. Res. **339**, 1711 (2004).
[45] F. Goubet, A. Ström, P. Dupree, and M. A. K. Williams, Carbohydr. Res. **340**, 1193 (2005).
[46] A. Ström and M. A. K. Williams, J. Phys. Chem. **107**, 10995 (2003).
[47] T. A. Waigh, Rep. Prog. Phys. **68**, 685 (2005).
[48] B. R. Dasgupta, S.-Y. Tee, J. C. Crocker, B. J. Frisken, and D. A. Weitz, Phys. Rev. E **65**, 051505 (2002).
[49] Y. Hemar and D. N. Pinder, Biomacromolecules **7**, 674 (2006).
[50] D. A. Weitz and D. J. Pine, in *Dynamic Light Scattering*, edited by W. Brown (Oxford University Press, Oxford, 1992).
[51] M. A. K. Williams, R. R. Vincent, D. N. Pinder, and Y. Hemar, J. Non-Newtonian Fluid Mech. (to be published).
[52] B. R. Dasgupta and D. A. Weitz, Phys. Rev. E **71**, 021504 (2005).
[53] S. Yamada, D. Wirtz, and S. C. Kuo, Biophys. J. **78**, 1736 (2000).
[54] Y. Tseng, J. S. H. Lee, T. P. Kole, I. Jiang, and D. Wirtz, J. Cell. Sci. **117**, 2159 (2004).
[55] F. K. Oppong, L. Rubatat, B. J. Frisken, A. E. Bailey, and J. R. de Bruyn, Phys. Rev. E **73**, 041405 (2006).
[56] C. Löfgren, S. Guillotin, and A.-M. Hermansson, Biomacromolecules **7**, 114 (2006).
[57] R. L. El Kossori, C. Villaume, E. El Boustani, Y. Savaire, and L. Mejean, Plant Foods Hum. Nutr. **52**, 263 (1998).